

# Spatio-temporally focused femtosecond laser pulses for nonreciprocal writing in optically transparent materials

Dawn N. Vitek,<sup>1</sup> Erica Block,<sup>1</sup> Yves Bellouard,<sup>2</sup> Daniel E. Adams,<sup>3</sup>  
Sterling Backus,<sup>4</sup> David Kleinfeld,<sup>5</sup> Charles G. Durfee,<sup>1</sup> and  
Jeffrey A. Squier<sup>1,\*</sup>

<sup>1</sup>Center for Micro-integrated Optics for Advanced Bio-imaging and Control, Department of Physics, Colorado School of Mines, Golden, Colorado 80401, USA

<sup>2</sup>Department of Mechanical Engineering, Eindhoven University of Technology, 5600 MB Eindhoven, The Netherlands

<sup>3</sup>Department of Physics and JILA, University of Colorado at Boulder and National Institute of Standards and Technology, Boulder, Colorado 80309, USA

<sup>4</sup>Kapteyn-Murnane Laboratories, Inc., Boulder, Colorado 80301, USA

<sup>5</sup>Department of Physics, University of California at San Diego, La Jolla, California 92093, USA

[\\*jsquier@mines.edu](mailto:jsquier@mines.edu)

**Abstract:** Simultaneous spatial and temporal focusing (SSTF) provides precise control of the pulse front tilt (PFT) necessary to achieve nonreciprocal writing in glass wherein the material modification depends on the sample scanning direction with respect to the PFT. The PFT may be adjusted over several orders of magnitude. Using SSTF nonreciprocal writing is observed for a large range of axial focal positions within the sample, and nonreciprocal ablation patterns on the surface of the sample are revealed. Further, the lower numerical aperture (0.03 NA) utilized with SSTF increases the rate of writing.

© 2010 Optical Society of America

**OCIS codes:** (140.3390) Laser materials processing; (050.2555) Form birefringence; (050.6624) Subwavelength structures; (050.6875) Three-dimensional fabrication; (230.4000) Microstructure fabrication; (190.4360) Nonlinear optics, devices.

---

## References and links

1. X. C. Wang, H. Y. Zheng, C. W. Tan, F. Wang, H. Y. Yu, and K. L. Pey, "Femtosecond laser induced surface nanostructuring and simultaneous crystallization of amorphous thin silicon film," *Opt. Express* **18**, 19379–19385 (2010).
2. Y. Shimotsuma, M. Sakakura, K. Miura, J. Qiu, P. G. Kazansky, K. Fujita, and K. Hirao, "Application of femtosecond-laser induced nanostructures in optical memory," *J. Nanosci. Nanotechnol.* **7**, 94–104 (2007).
3. J. W. Chan, T. Huser, S. Risbud, and D. M. Krol, "Structural changes in fused silica after exposure to focused femtosecond laser pulses," *Opt. Lett.* **26**, 1726–1728 (2001).
4. L. Sudrie, M. Franco, B. Prade, and A. Mysyrowicz, "Study of damage in fused silica induced by ultra-short ir laser pulses," *Opt. Commun.* **191**, 333–339 (2001).
5. E. Bricchi, B. G. Klappauf, and P. G. Kazansky, "Form birefringence and negative index change created by femtosecond direct writing in transparent materials," *Opt. Lett.* **29**, 119–121 (2004).
6. Y. Shimotsuma, P. G. Kazansky, J. Qiu, and K. Hirao, "Self-organized nanogratings in glass irradiated by ultrashort light pulses," *Phys. Rev. Lett.* **91**, 247405 (2003).
7. C. Hnatovsky, R. S. Taylor, P. P. Rajeev, E. Simova, V. R. Bhardwaj, D. M. Rayner, and P. B. Corkum, "Pulse duration dependence of femtosecond-laser-fabricated nanogratings in fused silica," *Appl. Phys. Lett.* **87**, 014104 (2005).

8. W. Yang, E. Bricchi, P. G. Kazansky, J. Bovatsek, and A. Y. Arai, "Self-assembled periodic sub-wavelength structures by femtosecond laser direct writing," *Opt. Express* **14**, 10117–10124 (2006).
9. G. Cheng, K. Mishchik, C. Mauclair, E. Audouard, and R. Stoian, "Ultrafast laser photoinscription of polarization sensitive devices in bulk silica glass," *Opt. Express* **17**, 9515–9525 (2009).
10. M. Beresna and P. G. Kazansky, "Polarization diffraction gratings produced by femtosecond laser nanostructuring in glass," *Opt. Lett.* **35**, 1662–1664 (2010).
11. P. G. Kazansky, W. Yang, E. Bricchi, J. Bovatsek, A. Arai, Y. Shimotsuma, K. Miura, and K. Hirao, "'Quill' writing with ultrashort light pulses in transparent materials," *Appl. Phys. Lett.* **90**, 151120 (2007).
12. B. Pommellec, M. Lancry, J.-C. Poulin, and S. Ani-Joseph, "Non reciprocal writing and chirality in femtosecond laser irradiated silica," *Opt. Express* **16**, 18354–18361 (2008).
13. W. Yang, P. G. Kazansky, Y. Shimotsuma, M. Sakakura, K. Miura, and K. Hirao, "Ultrashort-pulse laser calligraphy," *Appl. Phys. Lett.* **93**, 171109 (2008).
14. K. Osvay and I. N. Ross, "On a pulse compressor with gratings having arbitrary orientation," *Opt. Commun.* **105**, 271–278 (1994).
15. D. N. Vitek, D. E. Adams, A. Johnson, P. S. Tsai, S. Backus, C. G. Durfee, D. Kleinfeld, and J. A. Squier, "Temporally focused femtosecond laser pulses for low numerical aperture micromachining through optically transparent materials," *Opt. Express* **18**, 18086–18094 (2010).
16. F. He, H. Xu, Y. Cheng, J. Ni, H. Xiong, Z. Xu, K. Sugioka, and K. Midorikawa, "Fabrication of microfluidic channels with a circular cross section using spatiotemporally focused femtosecond laser pulses," *Opt. Lett.* **35**, 1106–1108 (2010).
17. G. Zhu, J. van Howe, M. Durst, W. Zipfel, and C. Xu, "Simultaneous spatial and temporal focusing of femtosecond pulses," *Opt. Express* **13**, 2153–2159 (2005).
18. D. Oron, E. Tal, and Y. Silberberg, "Scanningless depth-resolved microscopy," *Opt. Express* **13**, 1468–1476 (2005).
19. M. A. Coughlan, M. Plewicki, and R. J. Levis, "Parametric spatio-temporal control of focusing laser pulses," *Opt. Express* **17**, 15808–15820 (2009).
20. C.-H. Hsu, D. D. Carlo, C. Chen, D. Irimia, and M. Toner, "Microvortex for focusing, guiding and sorting of particles," *Lab Chip* **8**, 2128–2134 (2008).
21. J. P. Golden, J. S. Kim, J. S. Erickson, L. R. Hilliard, P. B. Howell, G. P. Anderson, M. Nasir, and F. S. Ligler, "Multi-wavelength microflow cytometer using groove-generated sheath flow," *Lab Chip* **9**, 1942–1950 (2009).
22. Y. Bellouard, A. Said, and P. Bado, "Integrating optics and micro-mechanics in a single substrate: a step toward monolithic integration in fused silica," *Opt. Express* **13**, 6635–6644 (2005).

## 1. Introduction

Three-dimensional (3D) micro- and nanoscale patterning with femtosecond lasers continues to gain novel applications in fields such as micro- and optofluidics, lithography and electronics. Recently, surface nanostructuring by irradiation with femtosecond laser pulses improved the absorption efficiency of thin film silicon solar cells [1]. Additionally, nanostructuring in doped glass was shown to have optical switching capabilities and, with only 150 nm spacing between bits, has application in compact optical memory storage [2]. The type of modification obtained from femtosecond laser exposure depends on the material composition and laser parameters. It has been suggested that femtosecond laser material modification in transparent materials be divided into three categories. In order of increasing intensity, these are: (type 1) a smooth, positive change in the refractive index; (type 2) form birefringence with associated anisotropic scattering; and (type 3) void formation [3–5]. Type 2 modifications are perhaps the least exploited, yet investigations of these modifications have revealed remarkable properties including strong polarization sensitivity. The form birefringence arises from subwavelength periodic variations in the refractive index along the dimension of light propagation and perpendicular to the direction of the electric field [6–8]. These type 2 modifications were suggested by Cheng *et al.* as a candidate for a polarization-selective optical router [9]. Using an arrangement of type 2 structures, they selectively guided polarized light with the electric field parallel to that of the writing laser. Beresna and Kazansky created a polarization diffraction grating by writing adjacent lines of type 2 modifications with periodic rotation of the writing laser's electric field [10]. Under some conditions, type 2 modifications have the additional quality of dependence upon the sample's scanning direction in that the characteristics of the

modification change when the scan direction is reversed, in an effect called nonreciprocal or “quill” writing [11–13]. This occurs even in centrosymmetric materials [12]. To further illuminate nonreciprocal writing, Yang *et al.* characterized type 2 modifications in one laser scanning direction and type 3 modifications in the reverse direction [13]. This phenomenon is due to pulse front tilt (PFT) [11, 13]. Kazansky *et al.* theorized that the intensity gradient established across the focal spot by the presence of PFT acts to displace electrons in the plasma by virtue of the ponderomotive force [11]. The PFT in combination with the direction of the movement of the sample affects the trapping and displacement of the electrons resulting in directionally-dependent writing. In practice, PFT may be imposed on the laser beam by tuning the laser’s grating compressor and quantified by measurements with a GRENOUILLE [13]. However, any adjustment to the parallelism of the gratings produces *angular* dispersion that necessarily results in spatial and temporal distortions at focus [14]. Consequently, the conditions for generating PFT are not easily translated between systems, so that deciphering the effect of PFT on nonreciprocal writing is confounded.

We propose a method to obtain the conditions necessary for nonreciprocal writing in a controlled and reproducible manner by exploiting the PFT inherent to a simultaneous spatial and temporal focusing (SSTF) arrangement. In SSTF *lateral* spatial chirping is used to form a frequency-distributed array of low numerical aperture (NA) beamlets. A feature of SSTF is that out-of-focus nonlinear interactions are suppressed, facilitating femtosecond material modification in the bulk of substrates [15, 16]. Importantly, at focus, the frequencies overlap spatially and temporally, and the pulse is transform-limited in time as well as diffraction-limited in space [17, 18]. PFT is achieved without misalignment of the grating compressor and may be measured using scanning SEA TADPOLE [19] and simulated using Fourier pulse propagation [15, 19]. The magnitude of PFT is adjusted by changing the beam aspect ratio (i.e., the ratio of the spatially chirped beam dimension to the unchirped dimension). With our SSTF system we examined nonreciprocal writing with several orders of magnitude more PFT than was employed by Yang *et al.* [13], and we obtained somewhat different dependencies. For example, they noted that for focal depths outside of a narrow region, nonreciprocal writing vanished. We observed a relaxed depth-dependence, and with our SSTF system we showed nonreciprocal writing with type 3 modifications on the back surface of the sample where either dots or Chevron shapes (the shape of a ‘V’ character) were patterned, depending on the scanning direction. Finally, working at low NA (0.03) with the SSTF setup, compared to 0.5–0.8 NA used in previous studies, increases the interaction volume and may improve the production rate of these features.

## 2. Experimental methods

The experimental setup, measurements and simulations were described in Vitek *et al.* [15]. Briefly, 25  $\mu\text{J}$  pulses at 1 kHz were supplied from a Ti:Al<sub>2</sub>O<sub>3</sub> chirped pulse amplification system centered at 800 nm. The SSTF system consisted of two gratings (600 l/mm, Thorlabs, #GR25-0608) that spatially chirped and then collimated the pulses. The ray-tracing model in Fig. 1 was simplified by representing the gratings in transmission, although they were, in fact, reflective. The angle of incidence (36°) on the gratings and the grating separation (630 mm) were selected to minimize second- and third-order dispersion. The beam incident on the focusing optic, which was a 25 mm focal length, 90-degree off-axis parabola (Janos Technology, #A8037-175), measured 8.4 mm and 0.55 mm full-width at half maximum (FWHM) in the spatially chirped and unchirped dimensions, respectively. At focus the spot size was 35  $\mu\text{m}$  FWHM, giving a laser fluence of 0.88 J/cm<sup>2</sup>. The pulse width at focus was 74 fs FWHM.

Nonreciprocal writing was monitored for variations in the scanning depth, rate, and direction

and in the electric field polarization. The sample was a 500  $\mu\text{m}$  thick fused quartz microscope slide (No. 24963-1, Polysciences, Inc.). We scanned the sample parallel to and perpendicular to the PFT at rates ranging from 5  $\mu\text{m/s}$  to 50  $\mu\text{m/s}$ . The electric field polarization was oriented either parallel to or perpendicular to the scanning direction.

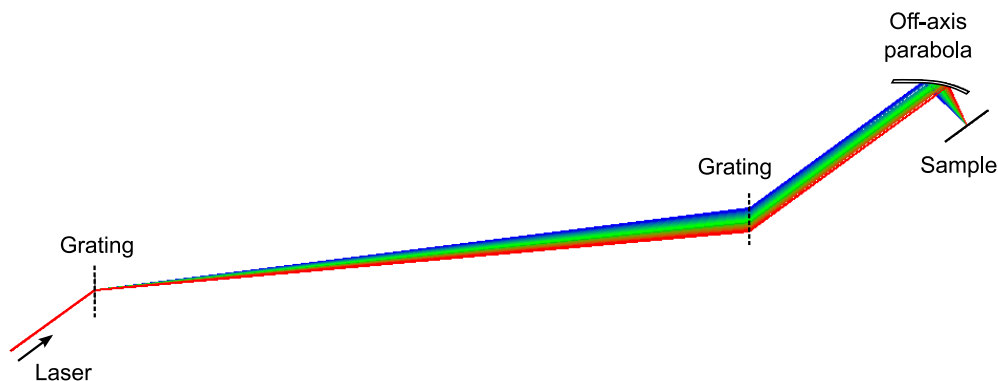


Fig. 1. Ray-tracing model of the SSTF system. Green, blue and red rays show the central wavelength and the FWHM edges of the spectrum, respectively.

### 3. Results and discussion

The PFT for our system was simulated by Fourier beam propagation [15]. The predicted value for the PFT at focus was 16,000 fs/mm [Fig. 2(a)], which is more than five orders of magnitude larger PFT than was employed by Yang *et al.* [13]. The simulation predicted that the PFT changes proportionally with the spatial chirp. We quantified the spatial chirp in a parameter called the beam aspect ratio (BAR). The BAR is the quotient of two length measurements: the beam width in the spatially chirped dimension with the beam with in the spatially unchirped dimension. For our system, the BAR was 15. With no applied spatial chirp and assuming a symmetric, circular input beam spot, the BAR = 1 and the PFT = 0. When spatial chirp was introduced, the PFT was predicted to increase linearly with the BAR [Fig. 2(b)].

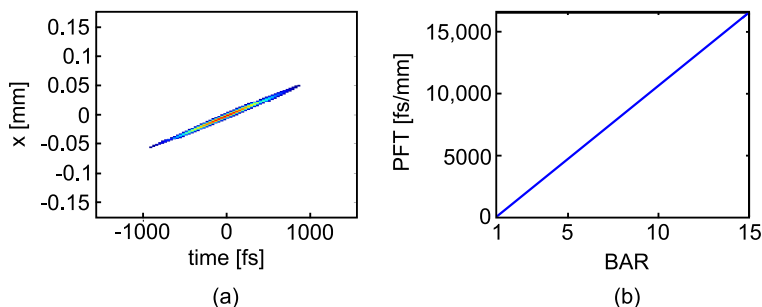


Fig. 2. (a) The simulated spatio-temporal intensity profile of the pulse at the focal plane where  $x$  is along the spatially chirped dimension. (b) The predicted relationship between the pulse front tilt (PFT) and the beam aspect ratio (BAR) for our system

Nonreciprocal writing was observed for scanning along the axis of PFT [Fig. 3(b) and 3(c)] but was not observed when scanning perpendicular to the PFT [Fig. 3(d)], supporting the claim that PFT causes nonreciprocal writing.

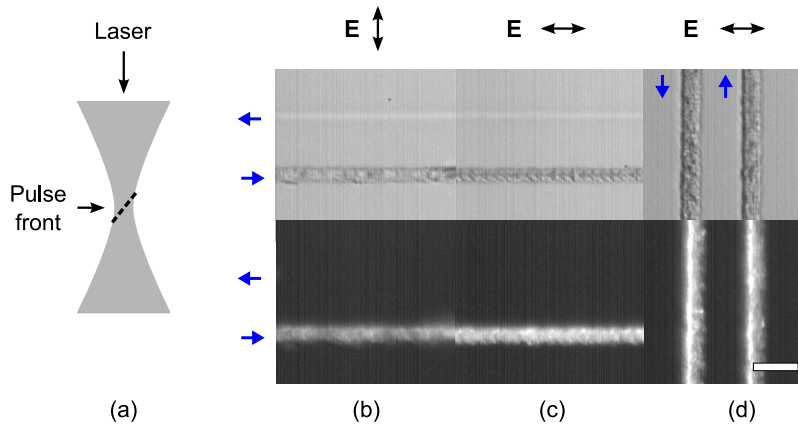


Fig. 3. (a) The orientation of the pulse front tilt at the focal plane (dashed line). The pulse arrives first on the left hand side of the focal spot. The scanning direction for the laser beam with respect to the sample for each written line in (b),(c) is indicated by blue arrows pointing to the left or the right. In (d) the scanning direction was perpendicular to the PFT. Each set of anti-parallel lines was imaged with bright field (top) and cross-polarized illumination (bottom). The orientation of the electric field,  $E$ , is marked with arrows in (b)–(d). The scanning rate was  $10 \mu\text{m/s}$ , and the location of the focal plane was  $284 \mu\text{m}$  beneath the surface of the sample. Scale bar,  $50 \mu\text{m}$ .

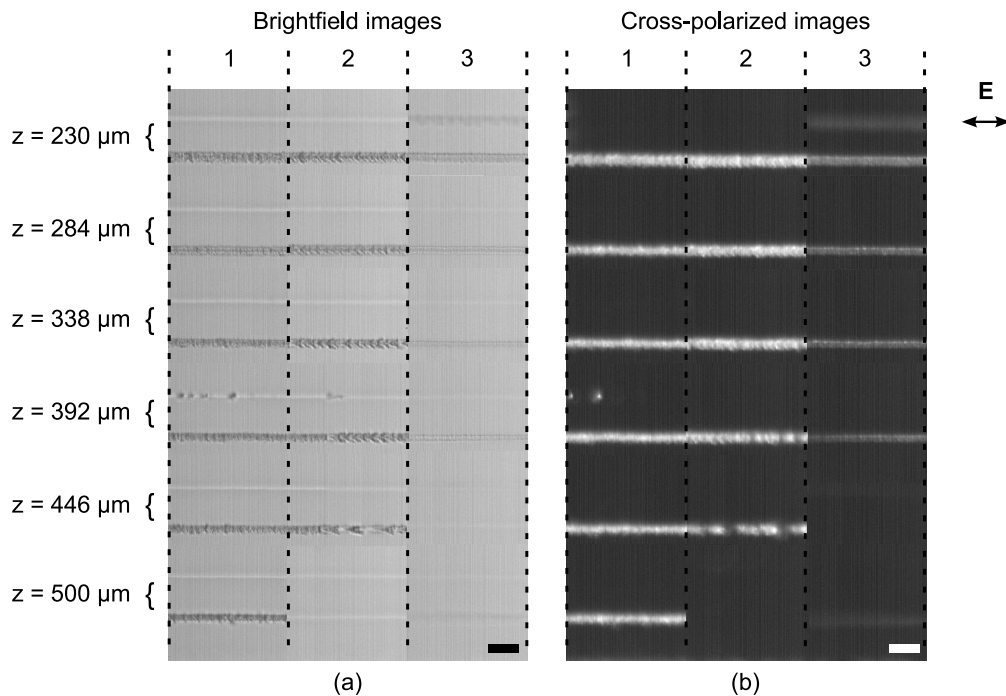


Fig. 4. Nonreciprocal writing was examined at different focal depths,  $z$ , beneath the surface of the sample. Each set of anti-parallel lines was imaged with (a) bright field and (b) cross-polarized illumination. The scan rates for regions 1, 2 and 3 were  $5 \mu\text{m/s}$ ,  $10 \mu\text{m/s}$  and  $50 \mu\text{m/s}$ , respectively. Scale bar,  $50 \mu\text{m}$ .

We observed nonreciprocal writing for focal positions ranging from 230  $\mu\text{m}$  to 500  $\mu\text{m}$  beneath the surface of the 500  $\mu\text{m}$  thick sample (Fig. 4). This is a much broader range than was seen by Yang *et al.* [13]. Under their experimental conditions (0.8 NA),  $\geq 5 \mu\text{m}$  movement in either direction eliminated the directional-dependence of the writing.

For focal positions  $\pm 54 \mu\text{m}$  outside of the 230  $\mu\text{m}$  to 500  $\mu\text{m}$  range, ablation occurred on the nearest surface. Interestingly, damage on the back surface showed nonreciprocal behavior (Fig. 5). Regularly spaced, 25  $\mu\text{m}$  diameter wells were ablated in one direction. In the opposite direction Chevron-shaped structures were produced. The spacing of the structures showed a small but not proportionate increase when the scan rate was doubled from 5  $\mu\text{m}/\text{s}$  to 10  $\mu\text{m}/\text{s}$  between regions 1 and 2. For the highest scan rate of 50  $\mu\text{m}/\text{s}$ , the structures became irregular. Organized surface patterning may find novel applications for femtosecond laser fabrication. For example, herringbone or Chevron-shaped structures have assisted with particle alignment in microfluidic channels by modifying the flow dynamics [20, 21]. Also, surface patterning provides additional functionalities for femtosecond laser processing of microelectromechanical systems (MEMS) [22].

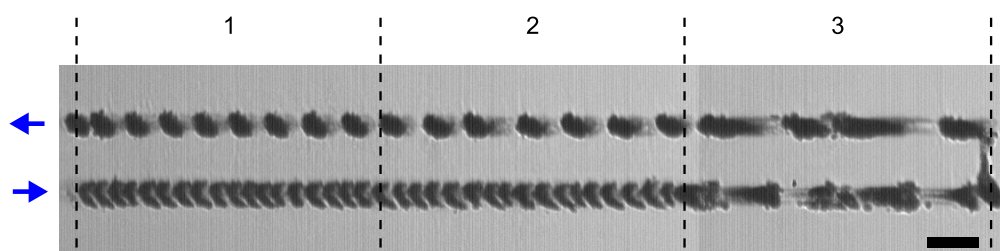


Fig. 5. Wells (top) or Chevron structures (bottom) were ablated for anti-parallel scanning directions on the back surface of the sample. The scan rates for regions 1, 2 and 3 were 5  $\mu\text{m}/\text{s}$ , 10  $\mu\text{m}/\text{s}$  and 50  $\mu\text{m}/\text{s}$ , respectively. The laser's electric field was oriented along the scanning direction. The blue arrows coincide with the orientation described in Fig. 3. Scale bar, 50  $\mu\text{m}$ .

#### 4. Conclusion

With an SSTF system, the PFT necessary in nonreciprocal writing is achieved in a calculable and reproducible manner and without the need to misalign the laser's grating or prism compressor. The SSTF system, having several orders of magnitude larger PFT and much lower NA, maintained nonreciprocal writing over a greater range of focal depths (230  $\mu\text{m}$  to 500  $\mu\text{m}$ ), including the back surface of a 500  $\mu\text{m}$  thick sample, and at more than two orders of magnitude less fluence than reported by previous work. Notably, the structures we have created here are of sufficient extent that patterned microfluidic channels can be created in a single pass. Thus, devices can be fabricated quickly and efficiently.

#### Acknowledgments

We thank Mariana Potcoava for her assistance with imaging. D. Vitek, J. Squier, S. Backus, and C. Durfee gratefully acknowledge support for this work from the Air Force Office of Scientific Research (AFOSR) (FA9550-07-10026 and FA9550-10-C-0017). J. Squier, E. Block and D. Kleinfeld acknowledge support from the National Institutes of Health (NIH) (EB003832).